Yonsei Medical Journal
Vol. 47, No. 2, pp. 214 - 222, 2006

In Vitro & *In Vivo* Effect of Parathyroid Hormone Analogue (1-14) Containing α-amino-iso-butyric Acid Residue (Aib)[1,3]

Yumie Rhee,[1] Weontae Lee,[2] Eun Jin Lee,[1] Suhyun Ma,[2] So Young Park,[1] and Sung-Kil Lim[1]

[1]Department of Internal Medicine, Endocrine Research College of Medicine, [2]Department of Biochemistry, College of Science, Yonsei University, Seoul, Korea.

Firstly, parathyroid hormone (1-14) [PTH (1-14)] analogue containing various α-amino-iso-butyric acid residue (Aib) was synthesized by exchanging the 1st and 3rd Ala residues of alpha carbon of PTH (1-14). This analogue revealed to have the quite tight and stable α-helical structure using the nuclear magnetic resonance (NMR) analysis. The biological activities of these analogues were examined using a cAMP-generating assay in LLC-PK1 cell lines stably transfected with the wild- type human PTH1 receptor. Only the PTH analogue substituted with methyl moiety without acetylation showed significant cAMP generating action with 15.0 ± 3.414 of EC_{50}. Then, we used an ovariectomized rat model system to compare the *in vivo* effects of parathyroid hormone analogue with that of PTH (1-84). Daily subcutaneous administration of the unacetylated Aib[1,3]PTH (1-14) for 5 weeks in 30 nM/kg subcutaneously with positive control group receiving PTH (1-84) with 8 nM/ kg were performed. However, there was no significant change in spinal or femoral bone mineral density assessed by dual x-ray absorptiometry (DXA) in the Aib[1,3]PTH (1-14) group where definite increase of these parameters shown in the PTH (1-84) group ($p < 0.001$). Assessment of bone strength was evaluated with no significant differences among all groups. It was quite disappointing to see the actual discrepancies between the result of significant pharmacokinetic potency and the *in vivo* clinical effect of the Aib[1,3]PTH (1-14). However, there are several limitations to mention, such as the short duration of treatment, matter of dosage, and insufficient effect of tight α-helical structures with absence of C-terminus. In conclusion, our findings suggest that unacetylated Aib[1,3]PTH (1-14) did not exhibit any anabolic effects at the bones of ovariectomized rats.

Key Words: Parathyroid hormone analogue, α-helical structure, ovariectomized rat, bone mineral density, bone strength

INTRODUCTION

Osteoporosis is a disease characterized by deteriorated bone strength which will finally lead to increased bone fragility and consequent increased risk of fractures.[1] Current available therapy for the treatment of osteoporosis is based on inhibition of bone resorption to prevent further bone loss. As there is substantial limitation of these anti-resorptives based on that there is already significant loss of bone, need for drugs that will stimulate bone formation existed. Low dose, intermittently administered parathyroid hormone (PTH) has recently approved by Food and Drug Administration (FDA) in year 2002. PTH causes a significant increase in bone mass in animals and humans, improves mechanical strength, and preserves trabecular bone connectivity in an animal model of osteoporosis.[2-7] However, there is still a practical problem regarding mode of administration. Only injection is available since the long peptide is degraded in the intestine.

The osteoblasts are the primary target cells for the anabolic effects of PTH on bone tissue. Binding of PTH to the seven-membrane spanning G-protein-coupled receptor and activation of both the 3,5-cyclic adenosine monophosphate (cAMP)-dependent protein kinase A (PKA) pathway and the phospholipase C-dependent protein kinase C pathway are the main signal streams to stimulate

Received July 28, 2005
Accepted November 15, 2005

This work was supported by research grants from the Korea Ministry of Health and Welfare (HMP- 01-PJ1-PG1-01CH08-0001) and Brain Korea 21 Project for Medical Science.

Reprint address: requests to Dr. Sung-Kil Lim, Department of Internal Medicine, College of Medicine, Yonsei University, #134 Shinchon-dong, Seodaemun-gu, Seoul 120-752, Korea. Tel: 82-2-2228-1973, Fax: 82-2-392-5548, E-mail: lsk@yumc.yonsei.ac.kr

the osteoblasts.[8] The mechanisms of the anabolic action of PTH are still not completely understood. However, referring to the previous *in vivo* studies using the N-terminal-truncated PTH fragment, which lacks PKA activity stimulation of cAMP production, failed to show the anabolic effect of PTH.[8-10] This indicates that this particular region with the subsequently activated cAMP pathway is the critical portion in the anabolic effect of PTH. Therefore using shorter PTH analogue contating critical portion will be useful in both aspect of the effect and possible convenient oral administration.

The amino-terminal portion is critical for PTH and PTH-related peptide (PTH/PTHrp) receptor activation.[11,12] N-terminus of PTH (1-14) weakly stimulated cAMP formation, about 10^{-3} folds of PTH (1-34) in LLC-PK cells stably expressing a high level of the hPTH/PTHrp receptor.[13] Substituted PTH analogues of each residue were analyzed subsequently. The short amino-terminal peptides of PTH, with various residues changed, could possibly be optimized to significantly increase signaling potency by modifying the interactions involving receptor regions containing the trans-membrane domains and the extra-cellular loops.[14,15] PTH (1-14) is regarded as the basic entity required for receptor activation, but the functionality of PTH (1-14) required for PTH/PTHrp receptor activation is retained in the first 9 amino acids.[15]

The previous extensive study on the structural and functional study on the various forms of PTH analogue was done. PTH (1-12) or PTH (1-11) with variable amino acid changes lead the different α-helical structure with significant effect on cAMP production level.[16] As the side chain and the alpha-helical structure seemed important, the newly formulated PTH analogue was composed of N-terminal 14 amino acid with especially substituted 1st amino acid to the moiety containing the α-amino-iso-butyric acid residue (Aib)[1,3] form from alanine residue. To confirm whether this specifically modified analogue, Aib[1,3] PTH (1-14), was effective *in vitro* and *in vivo*, this agent was tested on the production of cAMP and administered in the ovariectomized rat model analyzing the bone density and bone strength.

MATERIALS AND METHODS

Materials-peptide synthesis

The peptides used in this study were synthesized at Korea Basic Science Institute (Seoul, Korea) using the solid phase approach and they were purified by high performance liquid chromatography (HPLC). Peptide sequences were assembled with Milligen 9050 (Fmoc Chemistry). For deprotection, reagent mixture (88% trifluoroacetic acid, 5% phenol, 2% triisopropylsilane, 5% H_2O; 2 h) was used. The raw peptides were purified by HPLC (Delta PAK 15μ C18 300Å 3.9 × 150 mm column), with a 240 nm detector. Mass spectroscopy was used to confirm the molecular masses of the synthesized peptides.

cAMP generating assay

PTH receptor was stably expressed in the LLC-PK1 porcine kidney cells as previously described.[16] LLC-PK1 cells expressing the receptors were grown to confluence in 48-well plates. Cell culture medium was changed to complete Medium-199 containing 3% FBS 3-4 hrs before the cells were treated with peptides. For the assays, the medium was first removed and the cells were washed with 0.25 mL of cAMP-generating medium containing 3% FBS, 2 mM 3-isobutyl-1-methyl-xanthine, 0.1% BSA, 20 mM HEPES, and 0.002% ascorbic acid in complete Medium-199. cAMP-generating media (0.15 mL) containing various concentrations of peptides were added and the cells were incubated for 30 mins at 37℃. The media was then completely discarded, and the cells frozen at -70℃ for 30 min and thawed at room temperature for 15-20 min; this freeze-thawing process was repeated twice. The cells were then detached from the plates with 0.5 mL of 50 mM HCl solution per well, transferred to a 1.5 mL Eppendorf tube and centrifuged at 1900 × g for 10 min. The supernatants were then diluted 50-fold with radio-immunoassay (RIA) buffer and the cAMP concentration was measured using a cAMP ^{125}I RIA Kit (Stoughton, MA, USA), according to the manufacturer's instructions. The mean values of the data were fitted to a sigmoid curve with a variable slope

factor using the nonlinear squares regression technique in the GRAPHPAD PRISM. EC_{50} (nM) values are represented by means ± SE. All of the cAMP assays were performed in triplicate wells and repeated twice. ($p<0.05$ was considered significant).

NMR spectroscopy and modeling calculations

All NMR experiments are carried out in 70% H_2O (D_2O)/30% 2,2,2-trifluoro-(d_3)-ethanol (TFE) and 90%H_2O/10% D_2O at pH 7.2. The concentration was 1.5 mM in 50mM phosphate buffer. NMR spectra were acquired at 288K on a Bruker DRX-500 spectrometer (Rheinstetten, Germany) equipped with a triple resonance probe, and triple axis gradient coils. The spectra were also recorded over the temperature range 10-25℃, to calculate the temperature coefficients. Pulsed-field gradient (PFG) techniques were used in all H_2O experiments to suppress solvent signals. Two-dimensional total correlation spectroscopy (TOCSY),[17] with an MLEV-17 mixing pulse of 69.7 ms, and twodimensional (2-D) nuclear overhauser effect spectroscopy (NOESY),[18] with mixing times of 100-600 ms, was also performed. Two-dimensional double-quantum-filtered correlated spectroscopy (DQF-COSY)[19] spectra were collected in H_2O to obtain the vicinal coupling constants. NMR data were processed using XWIN-NMR (Bruker Instruments) software, and the processed data further analysed using sparky 3.60 software. Starting structures were generated using distance geometry (DG) by employing a refinement protocol using distance restraints assigned as strong, medium, or weak, on the basis of cross-peak volumes in the NOESY spectra. The dihedral angle constraints were also deduced from the $^3J_{HN\alpha}$ coupling constants from the 2-D DQF- COSY spectra in H_2O. Structure calculations were performed using hybrid distance geometry and the dynamically simulated-annealing (SA) protocol[20-23] using the CNS ver. 2.0.[24]

Animals and treatment

Thirty-six, five-month-old, virgin female Sprague-Dawley rats were purchased from the Department of Laboratory Animal Medicine at Yonsei Medical Research Center (Seoul, Korea). They were housed in a room maintained at 22.2℃ with 12-h light and 12-h dark cycles. The animals were fed freely with Purina laboratory rodent chow (Hagribrand Purina Korea Co., Kunsan, Korea), which contained 1.17% calcium, 0.77% phosphorous and 2.6 IU vitamin D per gram. All animals were treated in accordance with the guidelines and regulations for the use and care of animals of Yonsei University, Seoul, Korea.

Experimental design

The animals were randomized into the following four groups at the age of 9 weeks, with seven rats per group, and four rats were housed per cage. They were all ovariectomized (ovx) at the age of 10 weeks except the sham group. All the rats were left without any treatment for further 4 weeks. The first sham group and ovx group were treated with a vehicle (0.9% normal saline) for 5 weeks from the age of 14 week. All the rats in the remaining 2 groups were treated subcutaneously with recombinant human PTH (1-84) (rhPTH (1-84), 8 nM/kg) and $Aib^{1,3}$PTH (1-14) (30 nM/kg) for 5 weeks, respectively. The rhPTH (1-84), kindly donated by the Mogam Biotechnology Research Institute (Kyungi, Korea), was dissolved in 0.9% normal saline. $Aib^{1,3}$PTH (1-14) was also dissolved in 0.9% normal saline. At the end of the 5 weeks of treatment, the rats were sacrificed, and the femur and vertebrae were harvested and stored in saline-soaked gauze at -20℃ until required for analysis.

Bone densitometry

The bone mineral density (BMD) of the excised lumbar spine and right femora was measured by dual energy X-ray absorptiometry (DXA) (QDR-4500A, Hologic, Waltham, MA, USA). The specific bone was scanned at a resolution of 0.5 mm with a scanning speed of 2 mm/sec. The region was analyzed for bone mineral content (BMC), projected bone area and BMD. The triplicate determinations of the five different femora, with repositioning, showed a coefficient of the variation at 0.59%.

Femoral length and cross-sectional diameter at mid-diaphysis

The left femur lengths were measured using a Mitutoyo digital caliper (Cole Parmer, Vernon Hills, IL, USA). The femoral length was measured from the greater trochanter to intercondylar fossa. The length at the anterior-posterior (AP) and medial-lateral (ML) positions were measured.

Mechanical testing

The femurs were thawed prior to testing, and the bone strength of the intact femurs was measured using a three-point bending test. A load was applied midway between two supports that were 15 mm apart. The femurs were positioned so the loading point was 7.5 mm proximal from the distal popliteal space, and bending occurred about the medial-lateral axis. Load-displacement curves were recorded at a crosshead speed of 1 mm/sec using a servo-hydraulic materials testing machine (Instron LTD, Buckinghamshire, England) and an X-ray recorder (Hewlett Packard 7090A, Palo Alto, CA, USA).

Statistical analysis

All data were expressed as the means and standard deviation. SPSS 10.0 software (Chicago, Illinois, USA) was used for the statistical analysis. The differences in the BMD, cortical diameter and length, and various biomechanical data between the groups were compared using ANOVA with a Bonferroni's multiple group comparison procedure. A p value of less than 0.05 was accepted as statistically significant.

RESULTS

Schematic structures of PTH analogues

Basic chemical structure of PTH (1-14) in the 1st and 3rd Ala residues of alpha carbon is shown in Fig. 1A. These two sites were substituted with various moieties such as methyl, ethyl or propyl moieties (Fig. 1B).

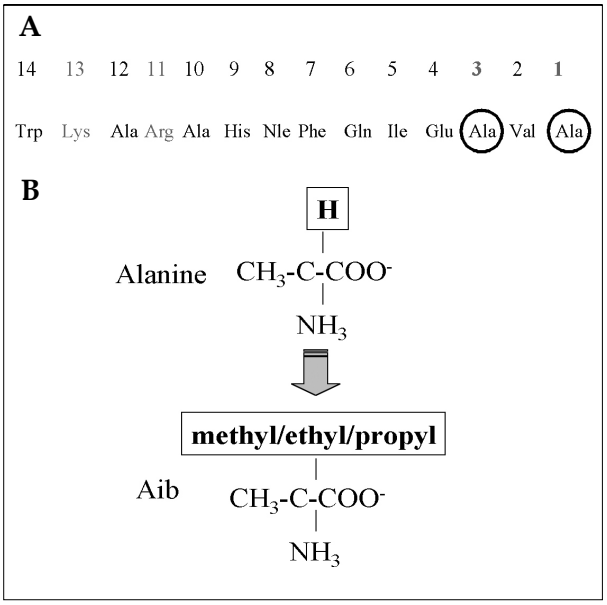

Fig. 1. Schematic structures of PTH analogs.

Biological effect of substitution in the 1st, 7th and 8th residues *in vitro*

Substitution of Ala^1 by methyl moiety substituted with ethyl or propyl moiety in Ala^1 showed no activity in cAMP generation (Fig. 2A). However, substitution of Ala1 by methyl moiety with unacetylation preserved cAMP production; however, acetylation of this analogue remarkably reduced cAMP accumulation (Fig. 2B).

Resonance assignment and NMR solution structure

To examine structure-function relationship of N-terminal acetylation of PTH (1-14), we determined solution structure of the $Aib^{1,3}$PTH (1-14). All resonance assignments of proton were possible using the standard sequential resonance assignment procedure.[25] As Aib moiety has no amide proton, it was assigned indirectly using NOESY spectra. As a consequence of NOE assignment and structure calculation, $Aib^{1,3}$PTH (1-14) shows a tight α-helical structure. A number of continuous stretch of intense $d_{NN}(i,i+1)$ NOEs are detected (Fig. 3). There are other short range dNN NOEs, supporting its helical structure (data not shown). To confirm the helical structure of $Aib^{1,3}$PTH (1-14), we displayed summary of the

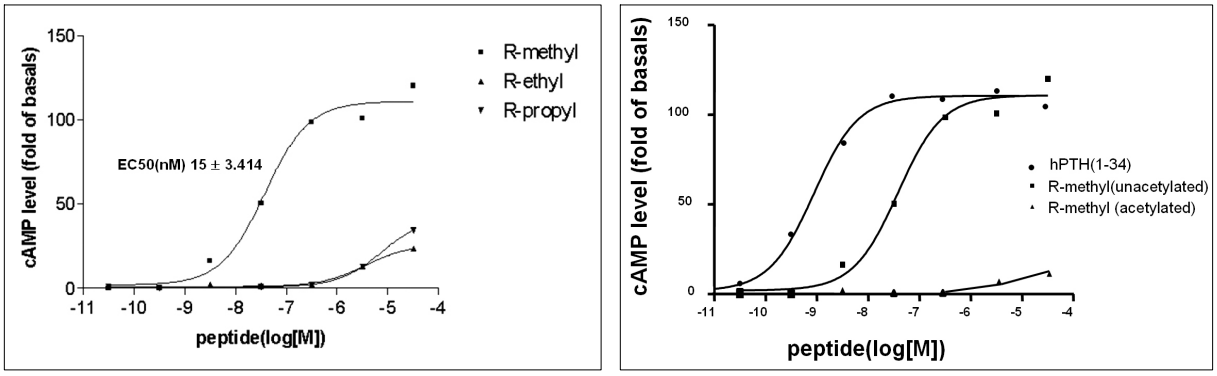

Fig. 2. cAMP formation of various PTH analogues in LLC-PK1 cells stably transfected with hPTH1R. (A) The effect of 1st and 3rd residue substitution in PTH (1-14) with methyl, ethyl and propyl moiety on cAMP activity. (B) The effects of acetylation in the AiBPTH (1-14) analogue. Each experiment was performed in duplicate and repeated three times. The symbols are defined in the figure key, and the curves were fitted to the data points by non-linear regression analysis, as described in Materials AND Methods.

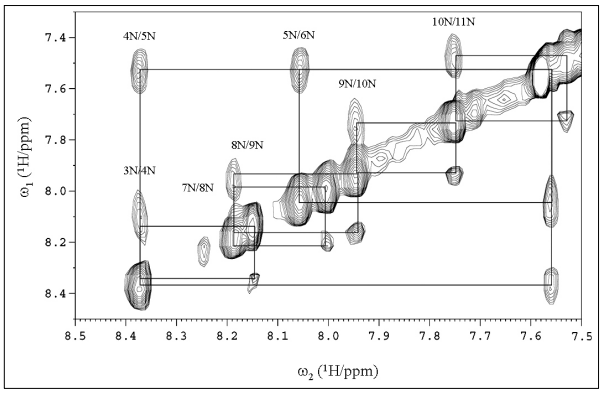

Fig. 3. Two-dimensional NOESY spectrum of modifications of PTH (1-14) showing NH regions with a mixing time 400 ms. Modification PTH (1-14) dissolved in 30% TFE solution at pH 7.2, 288 K. A continuous stretch of sequential d_{NN} (*i*, *i*+1) NOEs is observed in the helical region.

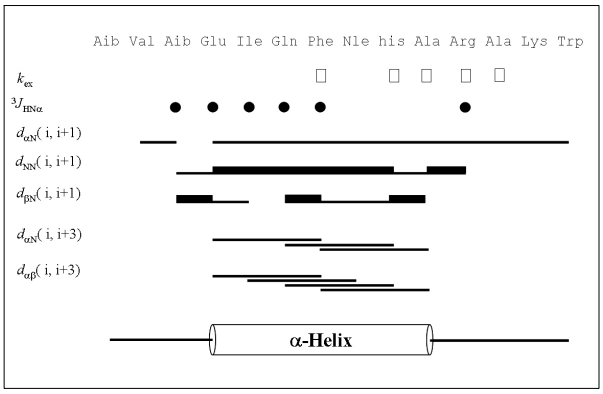

Fig. 4. Summary of NMR data for modifications of PTH (1-14) collected in 30% TFE solution at 288 K, showing the sequential and short-range NOE contacts. Slowly exchanging amide protons (□), backbone vicinal coupling constants (●; $^3J_{HN}$(<6 Hz), and chemical shift indices (CSI) for the $C_{\alpha H}$ chemical shift are indicated.

NMR data in aqueous 30% TFE condition (Fig. 4). The $d_{\alpha N}$ (*i*,*i*+1) as well as $d_{\alpha\beta}$ (*i*,*i*+3) and $d_{\alpha N}$ (*i*,*i*+1) NOEs also support α-helical structure of Aib[1,3] PTH (1-14), especially residues from Glu[4] to Ala[10].

The NMR structure was calculated using the experimental restraints derived from 2D-NOESY and DQF-COSY spectra. The 50 DG structures served as starting structures for dynamical simulated-annealing calculation. None of the 50 structures showed restraint violations > 0.05 nm for distances and 5° for torsion angles. The 15 lowest energy structures (<SA>$_k$) were selected from the 50 simulated-annealing structures for further structural analysis. The average structure (<SA>$_k$) was calculated from the geometrical average from 15 <SA>$_k$ structure coordinates and was subjected to restraint energy minimization (REM) to correct covalent bonds and angle distortions. Final 15 structures, superimposed upon the energy-minimized average structure and ribbon diagram REM structure are displayed (Fig. 5). The main α-helical region, Glu[4] to Ala[10] is compatible with NOEs and other NMR derived data. Considering the features of secondary structure, we can conclude that acetylation of the amino terminus does not make a critical effect on secondary structure of PTH (1-14) peptide. This conclusion is also consistent with the result that activities of cAMP formation of native PTH (1-14) and Aib[1,3]PTH (1-14) have no significant differences.

Skeletal effect of PTH analogue *in vivo*

After five weeks of injection, the excised lumbar spine (L1-L5) and right femur were analyzed by DXA. The BMC and BMD of the right femora were 7.2 and 5.2% lower and those of the lumbar spine were 3.0 and 7.6% lower in the ovx group respectively, than in the SHAM group (p<0.05) (Fig. 6A, 6B). Treatment of the ovx rats with rhPTH (1-84) for 5 weeks, resulted in a greater femoral and spinal BMD than in the ovx group (10.9% & 12.9%, respectively, p<0.001) In contrast, the rats administered with Aib^{1,3}PTH (1-14) showed no significant changes in BMD in both regions compared to ovx rats.

The femoral lengths after five weeks showed that in the groups treated with PTH (1-84) only showed significantly increased length (p<0.05) (Table 1).The femora diaphyses were evaluated with the three-point bending test at mid-shaft (Table 1). However, interestingly, there were no significant differences among all the groups treated nor untreated on the parameters such as, ultimate force (F_u), stiffness (S), ultimate stress (σ_u), Young's modulus (E) and toughness(u).

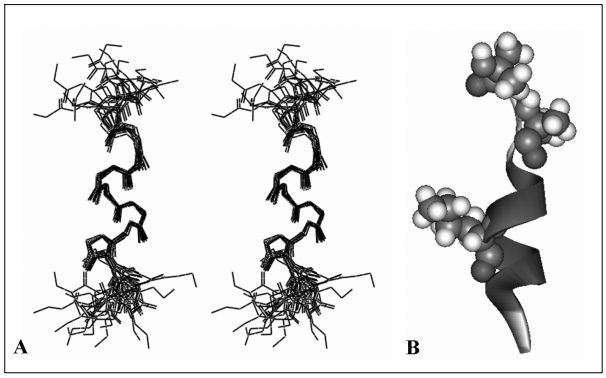

Fig. 5. Solution structures of Aib^{1,3} PTH (1-14). (A) Superimposition of the final 15 $<SA>_k$ structures of PTH (1-14) analogue upon the energy-minimized average structure ($<SA>_k$) (C^{α} traces) (B) Ribbon diagram of the PTH (1-14) analogue. Modified Aib^{1}, Aib^{3}, Nle^{8} residues are displayed using ball and stick model.

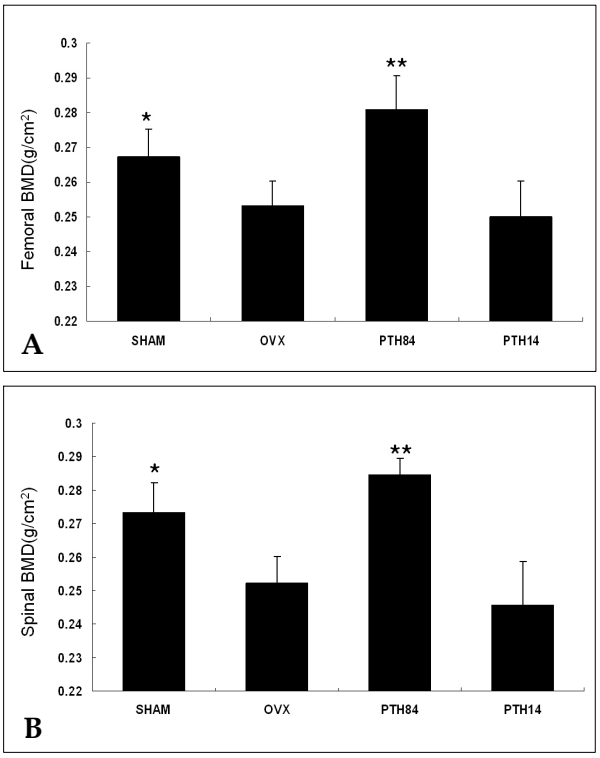

Fig. 6. Bone mineral density (BMD, g/cm^2) of the right femur (A). *p<0.05 vs. PTH14, **p<0.001 vs. OVX, PTH 14; lumbar spinal BMD (B); *p<0.005 vs. OVX, PTH14, **p<0.001 vs. OVX, PTH14.

Table 1. Anthropometric and Biomechanical Parameters of the Femora

	Length (mm)	AP (mm)	ML (mm)	F_u (N)	ε_u (mm)	U (N/mm^2)
SHAM	35.9/0.94	3.4/0.3	4.0/0.09	141.2/12.4	0.88/0.18	0.06/0.02
OVX	36.6/0.58	3.4/0.14	4.1/0.14	152.3/20.5	0.81/0.19	0.06/0.02
PTH84	**37.5/ 0.58***	3.4/0.20	4.0/0.12	149.3/8.4	0.79/0.19	0.06/0.02
PTH14	36.6/0.62	3.5/0.13	3.8/0.25	137.5/5.8	0.72/0.16	0.05/0.02

Data are shown as the mean ± SD.
The whole femoral length and the diameters of anterior-posterior and medio-lateral part of the mid-diaphysis are denoted in mm. The cortical bones of the femora diaphysis were examined using the three-point bending test to measure the ultimate force (Fu), ultimate strain (εu) and modulus of toughness (u).
*p<0.05 vs. OVX.

DISCUSSION

As the Aib residues are known to have a strong tendency to form type III β-bends, 310-helix increasing helicity, the Aib containing PTH (1-14) were synthesized around critical positions of 1st and 3rd positions of N-terminus.[26,27] The results of the conformational studies presented in this work show that the solution structure of unacetylated Aib[1,3] substituted PTH (1-14) analogues in the solvent system is characterized by tight helical segments. It was found that insertion of Aib residues at positions 1, 3 increased helicity in all tested peptides with consequent enhancement of potency and binding affinity.

Previous reports on the effect of shortened and modified PTH analogues *in vivo* have shown some of the significant effect compared to the FDA approved PTH (1-34). A lactam derivative of PTH (1-31)NH_2 itself also stimulates trabecular growth in the distal femurs of ovx rats as strongly as hPTH (1-34) only when injected at a high daily dose but it was only about 70% as effective as hPTH (1-34) when injected suboptimally.[28] Another report demonstrated that: PTH (1-31) was as potent as PTH (1-34) on the bone formation in mice but were less potent in stimulating bone resorption parameters in mice.[29] In addition there was difference degrees of increasing bone formation according to the site such as periosteal or endosteal region.[29] Therefore, these results indicate that the modified PTH analogues with similar biological potency might show quite different skeletal effect when administered *in vivo* system.

Data on the shorter PTH analogues are mainly on the *in vitro* biological potency and the structural-based analysis. For example, none of the 6/10 substituted analogues with linear or cyclic form remained as active as the parent peptide but the lactam-bridged analogues either maintained potency or showed 6-fold improvement.[30,31] Therefore, it is thought that an α-helical conformation of the N-terminal fragment of PTH and the structural order of the very first residues (1-4) of the signaling domain seemed critical in PTH action. NMR analysis on the unacetylated Aib[1,3] PTH (1-14) showed quite effective α-helical structure which was re-confirmed in the cAMP generating assay. However, contrary to the expectations usual acetylation of the peptide remarkably reduced the biological activity of the Aib[1,3] PTH (1-14). Thereafter, only the unacetylated Aib[1,3] PTH (1-14) was used in the following *in vivo* evaluation.

There were no significant changes in BMD or bone strength. The null effect of unacetylated Aib[1,3] PTH (1-14) in the ovx rat model was quite disappointing. However, these results indicate several important aspects of the modified short analogues of PTH. Firstly, the absence of C-terminus of the PTH which is thought to be quite important part in the effective signal transduction through the PTH receptor, might have significantly affected the anabolic effect even though there was good binding response of Aib[1,3] PTH (1-14) with the PTH receptor. The presence of the ordered two helical segments in the N-terminal and C-terminal is assumed to be essential for bioactivity. It means that the both of the activation and binding domains are important.[32] Secondly, our previous report and the recent reports by others, the α-helical structure of the PTH analogues are thought to be important in determining the activity by residue specificity in terms of optimum receptor pocket binding and helix stability.[16,31] However, it seems that only the tight and stable α-helical structure does not explain the whole biological effect of the modified analogues. Thirdly, the lysine and arginine residues of this Aib[1,3] PTH (1-14) might be the reason of null effect in that these residues are responsible for the peptide degradation, therefore, the action time of the Aib[1,3] PTH (1-14) could have been too short to show any effect with only once daily subcutaneous injection for 5 weeks. Lastly, the duration and the dosage of the Aib[1,3] PTH (1-14) might have been far short to show enough anabolic effect as was the case in the PTH (1-31)NH_2 in suboptimal dosage.[28]

In conclusion, the results of this study will assist in the understanding of the structure-biological activity relationships of short amino terminal oligopeptides, and this will provide a future direction for the development of effective low molecular weight PTH analogues. The proper direction of new substitution and cyclized analogues of PTH will lead to both for greater *in vitro* activity

and possibly for improved delivery and greater specificity as agents for restoration of bone loss in osteoporosis.

ACKNOWLEDGMENTS

We thank the Mogam Biotech. Institute (Sungnam, Korea) for providing the human PTH1R cDNA.

REFERENCES

1. Consensus development conference: prophylaxis and treatment of osteoporosis. Am J Med 1991;90:107-10.
2. Alexander JM, Bab I, Fish S, Muller R, Uchiyama T, Gronowicz G, et al. Human parathyroid hormone 1-34 reverses bone loss in ovariectomized mice. J Bone Miner Res 2001;16:1665-73.
3. Burr DB, Hirano T, Turner CH, Hotchkiss C, Brommage R, Hock JM. Intermittently administered human parathyroid hormone(1-34) treatment increases intracortical bone turnover and porosity without reducing bone strength in the humerus of ovariectomized cynomolgus monkeys. J Bone Miner Res 2001;16: 157-65.
4. Kneissel M, Boyde A, Gasser JA. Bone tissue and its mineralization in aged estrogen-depleted rats after long-term intermittent treatment with parathyroid hormone (PTH) analog SDZ PTS 893 or human PTH (1-34). Bone 2001;28:237-50.
5. Mashiba T, Burr DB, Turner CH, Sato M, Cain RL, Hock JM. Effects of human parathyroid hormone (1-34), LY333334, on bone mass, remodeling, and mechanical properties of cortical bone during the first remodeling cycle in rabbits. Bone 2001;28:538-47.
6. Sato M, Zeng GQ, Turner CH. Biosynthetic human parathyroid hormone (1-34) effects on bone quality in aged ovariectomized rats. Endocrinology 1997;138: 4330-7.
7. Neer RM, Arnaud CD, Zanchetta JR, Prince R, Gaich GA, Reginster JY, et al. Effect of parathyroid hormone (1-34) on fractures and bone mineral density in postmenopausal women with osteoporosis. N Engl J Med 2001;344:1434-41.
8. Kronenberg HM, Lanske B, Kovacs CS, Chung UI, Lee K, Segre GV,et al. Functional analysis of the PTH/ PTHrP network of ligands and receptors. Recent Prog Horm Res 1998;53:283-301; discussion 301-3.
9. Armamento-Villareal R, Ziambaras K, Abbasi-Jarhomi SH, Dimarogonas A, Halstead L, Fausto A, et al. An intact N terminus is required for the anabolic action of parathyroid hormone on adult female rats. J Bone Miner Res 1997;12:384-92.
10. Hilliker S, Wergedal JE, Gruber HE, Bettica P, Baylink DJ. Truncation of the amino terminus of PTH alters its anabolic activity on bone *in vivo*. Bone 1996;19:469-77.
11. Takasu H, Gardella TJ, Luck MD, Potts JT Jr, Bringhurst FR. Amino-terminal modifications of human parathyroid hormone (PTH) selectively alter phospholipase C signaling via the type 1 PTH receptor: implications for design of signal-specific PTH ligands. Biochemistry 1999;38:13453-60.
12. Juppner H, Schipani E, Bringhurst FR, McClure I, Keutmann HT, Potts JT Jr, et al. The extracellular amino-terminal region of the parathyroid hormone (PTH)/PTH-related peptide receptor determines the binding affinity for carboxyl-terminal fragments of PTH-(1-34). Endocrinology 1994;134:879-84.
13. Shimizu M, Potts JT Jr, Gardella TJ. Minimization of parathyroid hormone. Novel amino-terminal parathyroid hormone fragments with enhanced potency in activating the type-1 parathyroid hormone receptor. J Biol Chem 2000;275:21836-43.
14. Piserchio A, Bisello A, Rosenblatt M, Chorev M, Mierke DF. Characterization of parathyroid hormone/receptor interactions: structure of the first extracellular loop. Biochemistry 2000;39:8153-60.
15. Luck MD, Carter PH, Gardella TJ. The (1-14) fragment of parathyroid hormone (PTH) activates intact and amino-terminally truncated PTH-1 receptors. Mol Endocrinol 1999;13:670-80.
16. Lee EJ, Kim HY, Cho MK, Lee W, Lim SK. Structure and function of a minimal receptor activation domain of parathyroid hormone. Yonsei Med J 2004;45:419-27.
17. D.G. D, Bax A. Assignment of Complex ^{1}H NMR Spectra via Two-Dimensional Homonuclear Hartmann-Hahn Spectroscopy. J Am Chem Soc 1985;107:2820-1.
18. Jeener J, Meier BH, Bachman P, Ernst RR. Investigation of exchange processes by two-dimensional NMR spectroscopy. J Chem Phys 1979;71:4546-53.
19. Rance M, Sorensen OW, Bodenhausen G, Wagner G, Ernst RR, Wuthrich K. Improved spectral resolution in cosy 1H NMR spectra of proteins via double quantum filtering. Biochem Biophys Res Commun 1983;117:479-85.
20. Driscoll PC, Gronenborn AM, Beress L, Clore GM. Determination of the three-dimensional solution structure of the antihypertensive and antiviral protein BDS-I from the sea anemone Anemonia sulcata: a study using nuclear magnetic resonance and hybrid distance geometry-dynamical simulated annealing. Biochemistry 1989;28:2188-98.
21. Nilges M, Clore GM, Gronenborn AM. Determination of three-dimensional structures of proteins from interproton distance data by hybrid distance geometry-dynamical simulated annealing calculations. FEBS Lett 1988;229:317-24.
22. Nilges M, Clore GM, Gronenborn AM. Determination of three-dimensional structures of proteins from interproton distance data by dynamical simulated annealing from a random array of atoms. Circumventing problems associated with folding. FEBS Lett 1988;239:129-36.

23. Nilges M, Gronenborn AM, Brunger AT, Clore GM. Determination of three-dimensional structures of proteins by simulated annealing with interproton distance restraints. Application to crambin, potato carboxypeptidase inhibitor and barley serine proteinase inhibitor 2. Protein Eng 1988;2:27-38.
24. Brunger AT, Adams PD, Clore GM, DeLano WL, Gros P, Grosse-Kunstleve RW, et al. Crystallography & NMR system: A new software suite for macromolecular structure determination. Acta Crystallogr D Biol Crystallogr 1998;54:905-21.
25. Wuthrich K. NMR proteins and Nucleic Acids. New York: Wiley; 1986.
26. Karle IL, Balaram P. Structural characteristics of alpha-helical peptide molecules containing Aib residues. Biochemistry 1990;29:6747-56.
27. Bolin KA, Anderson DJ, Trulson JA, Thompson DA, Wilken J, Kent SB, et al. NMR structure of a minimized human agouti related protein prepared by total chemical synthesis. FEBS Lett 1999;451:125-31.
28. Whitfield JF, Morley P, Willick G, MacLean S, Ross V, Isaacs RJ, et al. Comparison of the abilities of human parathyroid hormone (hPTH)-(1-34) and [Leu27]-cyclo (Glu22-Lys26)-hPTH-(1-31)NH2 to stimulate femoral trabecular bone growth in ovariectomized rats. Calcif Tissue Int 1998;63:423-8.
29. Mohan S, Kutilek S, Zhang C, Shen HG, Kodama Y, Srivastava AK, et al. Comparison of bone formation responses to parathyroid hormone(1-34), (1-31), and (2-34) in mice. Bone 2000;27:471-8.
30. Shimizu N, Petroni BD, Khatri A, Gardella TJ. Functional evidence for an intramolecular side chain interaction between residues 6 and 10 of receptor-bound parathyroid hormone analogues. Biochemistry 2003;42: 2282-90.
31. Tsomaia N, Pellegrini M, Hyde K, Gardella TJ, Mierke DF. Toward parathyroid hormone minimization: conformational studies of cyclic PTH(1-14) analogues. Biochemistry 2004;43:690-9.
32. Condon SM, Morize I, Darnbrough S, Burns CJ, Miller BE, Uhl J, et al. The bioactive conformation of human parathyroid hormone. Structural evidence for the extended helix postulate. J Am Chem Soc 2000;122: 3007-14.